UMYU Scientifica, Vol. 4 NO. 4, December 2025, Pp 310 – 325
https://doi.org/10.56919/usci.2544.028
ISSN: 2955 – 1145 (print); 2955 – 1153 (online)
A periodical of the Faculty of Natural and Applied Sciences, UMYU, Katsina

ORIGINAL RESEARCH ARTICLE

Characterization and Antibacterial Activity of Endophytic *Aspergillus niger* strain MOR-1 Isolated from *Moringa oleifera*

Abdullahi Ibrahim Dalhatu[1], Bahauddeen Salisu[2]*, Mukhtar Gambo Lawal[2] and Hayatudeen Muhammad Rumah[2]

[1]Department of Microbiology, College of Natural and Applied Sciences, Al-Qalam University, PMB 2137, Katsina, Nigeria
[2]Department of Microbiology, Faculty of Science, Umaru Musa Yar'adua University, PMB 2218, Katsina, Nigeria

ABSTRACT

The increase in multidrug-resistant (MDR) microorganisms has driven the global search for new antimicrobial drugs from untapped natural sources. One of the biggest sources of bioactive secondary metabolites is endophytic fungi, symbiotic microorganisms that inhabit plant tissues. It is true that, despite the abundance of medicinal plant species in the state of Katsina, Nigeria, there is no scientific knowledge of the antibacterial potential of the endophytic fungi of these plants. Thus, this paper seeks to isolate and profile endophytic fungi towards new antibacterial derivatives. This study isolated *Aspergillus niger* from *Moringa oleifera*, and the exometabolites were extracted, and their antibacterial activity against 10 pathogenic bacterial strains was measured using the disc diffusion technique. The fungal extract was analyzed through Gas Chromatography-Mass Spectrometry (GC-MS), Fourier Transform Infrared Spectroscopy (FTIR), in silico molecular docking to estimate binding affinities with bacterial enzymes (ECPR, MurA, and PBPs), and Adsorption, Distribution, Metabolism, Excretion/Toxicity (ADME/T) to establish the drug likeness. The antibacterial assay showed that *the Aspergillus niger* strain MOR-1 exhibited broad and strong activity, with inhibitory diameters ranging from 16.67 ± 1.53 mm to 29.33 ± 2.52 mm against *S. aureus, P. aeruginosa, K. pneumoniae, S. pneumoniae, S. typhi*, and *E. coli*. The activity of the strain was similar to that of ciprofloxacin (12.10 ± 1.05 to 30.1 ± 0.41 mm), indicating the synthesis of effective antibacterial metabolites with broad-spectrum activity. Analysis of the fungal extracts by GC-MS revealed various bioactive compounds, including fatty acid esters, alcohols, phenols, and aldehydes with known antimicrobial properties. The presence of functional groups (including hydroxyl, carbonyl, and alkene groups) which are typical of bioactive secondary metabolites was further confirmed by FTIR spectroscopy. The molecular docking experiments indicated that the important compounds, especially methyl ricinoleate, 9-octadecenoic acid, and methyl linolenate, exhibit high binding affinity to essential bacterial target enzymes involved in cell wall and protein synthesis. The predicted pharmacokinetic and low-toxicity profiles of the lead compounds, based on ADME/T screening, supported their potential as drug-like antibacterial candidates. The results show that *Aspergillus niger* is a promising source of potent antibacterial metabolites with activities similar to those of standard antibiotics. Future research should focus on purifying and testing the most promising compounds *in vivo* to establish their therapeutic potential as new antibacterial agents.

ARTICLE HISTORY

Received September 03, 2025
Accepted December 19, 2025
Published December 30, 2025

KEYWORDS

Bacteria, GCMS, FTIR, Molecular docking, Antibacterial activity

INTRODUCTION

In recent years, there has been growing interest in fungal endophytes, a highly diverse group of microorganisms that inhabit plant tissues without causing visible harm to their host plants (Rai *et al.*, 2021). First described by Anton de Bary in 1866, endophytic fungi are now recognized as ubiquitous components of plant microbiomes, occurring in nearly all plant species across diverse climatic and ecological zones, including terrestrial and marine environments (Chakraborty *et al.*, 2021; Abdelaziz *et al.*, 2025). Although estimates may be exaggerated, it has been suggested that approximately one million endophytic fungal species exist globally, with particularly high diversity reported in tropical and subtropical regions (Bala *et al.*, 2025). Their occurrence and distribution are influenced by host plant species, geographical location, seasonal variation, and anthropogenic activities (Eo *et al.*,

Correspondence: Bahauddeen Salisu. Department of Microbiology, Faculty of Science, Umaru Musa Yar'adua University, PMB 2218, Katsina, Nigeria. ✉ bahauddeen.salisu@umyu.edu.ng.

How to cite: Ibrahim, A. D., Salisu, B., Gambo, M. L., & Muhammad, H. R. (2025). Characterization and Antibacterial Activity of Endophytic *Aspergillus niger* strain MOR-1 Isolated from *Moringa oleifera*. *UMYU Scientifica*, 4(4), 310 – 325. https://doi.org/10.56919/usci.2544.028

2022). While members of Basidiomycota and Zygomycota are present, the majority of endophytic fungi belong to the phylum Ascomycota (Lin *et al.*, 2023).

Endophytic fungi display remarkable ecological and functional versatility, existing as mutualists, latent pathogens, or former pathogens that have lost their virulence depending on host physiology and environmental conditions (Mishra *et al.*, 2021). This adaptability complicates their precise definition, particularly for unculturable species whose biological roles within host tissues remain unclear (Mattoo and Nonzom, 2021). Advances in metabolomics and next-generation sequencing have significantly improved the exploration of endophytic fungal diversity and biosynthetic potential, revealing these organisms as promising reservoirs of agriculturally and pharmaceutically important bioactive compounds (Bielecka *et al.*, 2022).

The renewed scientific interest in endophytic fungi is closely linked to the escalating global challenge of antimicrobial resistance (AMR), which threatens the continued effectiveness of conventional antibiotics (Tiwari *et al.*, 2025). The World Health Organization has identified AMR as one of the most critical public health threats of the twenty-first century, with resistant infections affecting millions of people annually and causing tens of thousands of deaths worldwide (Salam *et al.*, 2023). This alarming trend underscores the urgent need for innovative, effective, and low-toxicity antimicrobial agents, particularly those with novel mechanisms of action and reduced potential for resistance development (Elshobary *et al.*, 2025).

Secondary metabolites are structurally diverse, low-molecular-weight compounds produced by many organisms, particularly microorganisms, and they have historically played a central role in drug discovery (Buddhika and Abeysinghe, 2020). While plants have long been recognized as valuable sources of therapeutic agents (Dar *et al.*, 2023), microorganisms have gained prominence due to their vast biodiversity, rapid growth, and amenability to genetic and metabolic manipulation (Thiele-Bruhn, 2021). However, extensive exploration of soil-derived microorganisms has led to frequent rediscovery of known compounds, necessitating a shift toward alternative, underexplored microbial niches (MacNair *et al.*, 2023). In this regard, plant-associated microorganisms, particularly endophytic fungi, have emerged as promising alternative sources of chemically novel and biologically active secondary metabolites (Gakuubi *et al.*, 2021).

Endophytic fungi occupy a unique ecological niche within plant tissues, enabling intimate interactions with host metabolic pathways and facilitating the production of structurally diverse and novel compounds not commonly synthesized by free-living microorganisms (Chandra and Enespa, 2019). This shift in natural product research emphasizes the importance of previously overlooked ecological systems in the search for new antimicrobial agents (Aghdam and Brown, 2021). Due to their adaptive metabolic plasticity, endophytic fungi can produce a broad spectrum of secondary metabolites under varying physiological and environmental conditions, particularly when subjected to co-cultivation, stress induction, or optimized culture conditions (Wadhwa *et al.*, 2024).

The pharmaceutical relevance of endophytic fungi was notably highlighted by the discovery of Taxol production by *Taxomyces andreanae*, which transformed bioprospecting strategies and demonstrated the ability of endophytes to synthesize compounds previously believed to be plant-specific (Tripathi and Agnihotri, 2024). Beyond their medicinal value, endophytic fungi contribute significantly to host plant fitness by enhancing resistance to biotic and abiotic stresses such as drought, salinity, oxidative stress, heavy metal toxicity, and pathogen invasion (Verma *et al.*, 2022; Grabka *et al.*, 2022). These protective attributes further support their potential roles in sustainable agriculture and resistance management strategies (Tiwari and Bae, 2022).

Several classes of endophyte-derived metabolites, including alkaloids, polyketides, terpenoids, peptides, phenolics, and aliphatic compounds, have demonstrated potent antibacterial activity against a wide range of human pathogens (Das *et al.*, 2024). Some endophytic fungal strains have shown activity against multidrug-resistant pathogens such as *Pseudomonas aeruginosa*, *Escherichia coli*, and *Staphylococcus aureus*, positioning them as important candidates in the global fight against AMR (Eshboev *et al.*, 2024). Despite this potential, research on endophytic fungi remains relatively limited due to challenges in cultivation, metabolite isolation, and structural characterization (Adeleke and Babalola, 2021; Gakuubi *et al.*, 2021). Nonetheless, the integration of omics-based approaches, including genomics, transcriptomics, proteomics, and metabolomics, continues to reveal silent biosynthetic gene clusters with significant antibacterial potential (Hur *et al.*, 2023; Saini *et al.*, 2024).

Although several medicinal plants in Nigeria, including those from Katsina State, have been investigated for their antibacterial properties, comparatively little attention has been given to the endophytic fungi associated with these plants. Considering the ecological diversity of Katsina State and the medicinal relevance of its indigenous flora, endophytic fungi from this region represent an underexplored but promising source of novel antibacterial compounds.

Therefore, this study aims to isolate, characterize, and evaluate *Aspergillus niger* associated with *Moringa oleifera* from Katsina State, Nigeria, for the production of novel antibacterial compounds. The findings are expected to contribute to antimicrobial drug discovery and expand current knowledge on the taxonomic and ecological diversity of endophytic fungi in this region.

MATERIALS AND METHODS

Study Area

The study took place in Katsina State, in the north of Nigeria. The area of Katsina State is 23,938 square kilometres, and its latitude and longitude are 11°08'N 13°22'N and 6°52'E 9°20'E (Ibrahim *et al.*, 2022). The state consists of 34 Local Government Areas; it is bordered to the north by the Niger Republic; to the east by the Jigawa and Kano States; to the south by the Kaduna State; and to the west by the Zamfara State (Kankara and Abdullahi, 2024).

Collection of Plant Materials

Fresh leaves of *Moringa oleifera* were collected at the Biological Garden of Al-Qalam University, Katsina. After the process outlined by Shehu (2023), the plant leaf samples were packed into a plastic container and immediately transported to the laboratory. The samples were washed with warm water.

Isolation of Fungi

The plant leaves were first washed with sterile distilled water to remove any undesired dirt, as per the process employed by Qadri *et al.* (2013) and Zihad *et al.* (2022). They were then surface-sterilized with 75% ethanol, 0.5% sodium hypochlorite, and 75% ethanol, each for 1 and 3 minutes and 15 seconds, respectively, after proper washing with sterile distilled water. Then they were cut into minute pieces, about 0.5 cm2 in size, using a sharp, sterile blade, and placed on Petri dishes containing Potato Dextrose Agar (PDA) medium in a horizontal manner. 100 µg/mL streptomycin was added to the PDA medium to stop bacterial growth. Fungal colonies were cultured for 7 days in Petri dishes at room temperature. Colonies were sorted into groups based on their appearance, morphology, and color. A colony from the first culture plate was unique, so a small piece was transferred to form a pure culture. This was then spotted on Petri dishes containing PDA media that was supplemented with streptomycin. The incubation period of the plates was seven days.

Preparation of Crude Extract of Endophytic Fungal Isolate

The fungal extract was prepared using the method outlined by Zihad *et al.* (2022). The fungi in the pure culture plates were transferred to PDA slants and incubated for 48 hours at 30 °C to determine the growth stage of each fungus. The increasing size of each fungus was then transferred onto PDA slants in conical flasks containing 200ml autoclaved potato dextrose broth media at 121 °C for 15 minutes. The 10 days of culture in the flasks were conducted at 28 °C . The mycelial biomass was filtered using a Whatman No. 1 filter, followed by three withdrawals of the filtrate with an equal volume of ethyl acetate using a separating funnel. The extracts were pooled, and the mixture was rotary-evaporated at 400 °C to yield a crude, semisolid extract, after which it was dried into powder using a hot air ovum at 400C. The powdered extracts were kept in vial until needed for further analysis.

Evaluation of Antibacterial Activity of Crude Extract of Endophytic Fungal Isolate

Ten (10) bacterial isolates from the culture collection of the Microbiology Department of Al-Qalam University, Katsina; Umaru Musa Yar'adua University, Katsina; and Federal Teaching Hospital, Katsina were used for antibacterial screening. The following were collected: *Staphylococcus aureus, Pseudomonas aeruginosa, Klebsiella pneumoniae,* Methicillin-Resistant *Staphylococcus aureus* (MRSA), *Streptococcus pneumoniae, Salmonella typhi, Shigella* sp., *Citrobacter* sp. and *Escherichia coli* based on the list of antibiotic-resistant pathogens developed by the World Health Organization (WHO) that highlights the necessity of new antimicrobial drugs against high-risk and clinically important bacteria. The bacteria were grown in nutrient broth for 18 hours at 37 °C, after which the bacterial pellets were suspended in 5 mL of sterile normal saline and then centrifuged at 4000 rpm. The bacterial concentration was subsequently determined using the McFarland standard and diluted to an operational concentration of 5×10^6 cfu/mL.

The disc diffusion method was employed to test the antibacterial activity of crude endophytic fungal extracts (Lykholat *et al.*, 2021). A bacterial suspension (10^9 cfu) was placed on Petri dishes containing Mueller-Hinton Agar (MHA). The crude extract (100 µg) was placed on sterile 6 mm diameter paper discs on the agar. The plates were incubated for 24 hours at 37 °C. The positive control (5 µg per disc) was ciprofloxacin. Antibacterial activity of the extracts was assessed by measuring the diameter (mm) of the inhibition zones they formed. The antibacterial assay was used as a preliminary screening tool to select the most potent endophytic fungal isolate for subsequent identification and chemical characterization.

Identification of the Most Potent Endophytic Fungal Isolate

The identification of the most potent fungal isolate was carried out using an integrated procedure that combined cultural and microscopic analyses, as recommended by Abdelgawad *et al.* (2022), Zihad *et al.* (2022), and Salisu *et al.* (2024). Three days of culture growth were carried out on PDA plates at 25 °C. To initiate the morphological identification process, glass slides and cover slips were cleaned with 95% ethanol. The microscope slide was then sanitized, and a drop of lactophenol-cotton blue was added. A dye culture plate was prepared by adding a small piece of mycelium with a needle, then a cover slip was placed on the mycelium. The slide was observed under a light microscope using a 40x objective lens, and photographs were taken.

Molecular Characterization of the Most Potent Endophytic Fungal Isolate

Isolation of DNA

The Cetyltrimethylammonium bromide (CTAB) procedure described by Singh *et al.* (2020) was used to extract DNA from the fungal isolates. Mortars and pestles were pre-chilled to 4 °C, and 1 g of the sample was placed

in absolute alcohol for 30 minutes, after which the alcohol was left to evaporate. Then, 5 grams of the mycelium were crushed into a fine powder using a sterile mortar and pestle, and 10 mL of pre-warmed isolation buffer was combined with the crushed mycelium and stirred. Upon incubation, the mixture was allowed to cool to room temperature then 10 mL of the chloroform-isoamyl alcohol (24:1) was added and thoroughly mixed. The mixture was centrifuged at 10,000 rpm for 24 °C, after which the supernatant was transferred to a fresh sterile tube. Ice-cold isopropanol (0.6 volume) and 3 M sodium acetate (0.1 volume) were added to the aqueous layer, and the mixture was allowed to stand at -20 °C for 30 minutes. The mixture was centrifuged at 10,000 rpm for 10 minutes at 4^0C and the supernatant was discarded. The obtained DNA pellet was washed with 75% ethanol and centrifuged once again at 10000rpm for 10 minutes at 4 °C. The ethanol was decanted, and the DNA pellet was driedine air and suspended in 200 ul of distilled water.

Polymerase Chain Reaction (PCR) Amplification

Amplification of the ITS region of the rRNA operon was performed using the forward primer (ITS-1F), which is 5'-TCCGTAGGTGAACCTGCGG-3' and the reverse primer (ITS-4R), 5'-TCCTCCGCTTATTGATATGC-3' (Salisu *et al.*, 2024a). PCR amplification was performed at the Centre of Biotechnology, Bayero University Kano, using standard molecular biology procedures. Ration of each reaction mixture was 10 ul of Red Taq ready mix, 0.5 ul of each primer, 8 ul of sterile analytical-grade water (Sigma-Aldrich), and 5 ul of genomic DNA, 24 ul. The conditions used for thermocycling were denaturations at 94 °C for 5 min, followed by 30 cycles of denaturations at 94 °C for 1 min, annealing at 60 °C for 1 min, extension at 72 °C for 1 min, and finally an extension at 72 °C for 5 min. PCR products were separated on a 2% agarose contained on a Tris-acetate-EDTA buffer, stained with ethidium bromide, and visualized under UV light (Etanke *et al.*, 2021). The molecular weight marker used in estimating the amplicon sizes was a 1 kb Plus DNA ladder.

DNA Sequencing and BLASTs Analysis

The amplified samples were transported to South African Medical Research Council (SAMRC) Genomic Centre for sequencing. The received sequence data were processed using the BLAST (Basic Local Alignment Search Tool) algorithm (http://blast.ncbi.nlm.nih.gov) in the NCBI database for sequence alignment and identification.

Phylogenetic Relationship

The DNA sequences obtained during this study were analyzed to construct a phylogenetic tree using the neighbour-joining method in MEGA 12 (build: 12251022-x86_64; version 12.0.15).

Gas Chromatography Mass Spectrometry Analysis

The chemical structure of fungal extracts was determined using a gas chromatography-mass spectrometry (GC-MS) system (Shimadzu GC-MS-QP2010 Plus, Japan). The instrument had an AOC-20i autoinjector set to split injection mode. Before analysis, the syringe was washed 4 times with pre-solvent and post-solvent, and 3 times with the sample, to avoid contamination. The temperature of the injection port was kept at 200-250 °C, and the injection volume was 1 uL. The carrier was helium, operated in linear velocity flow control mode with a column flow rate of 1.8 mL/min, a total flow of about 40.8 mL/min, and a split ratio of 20:1.

The temperature of the column oven was adjusted to 70 °C and scheduled to increase to 280 °C at a rate of 10 °C/min and a hold time of 5 minutes. The interface temperature was kept at 250 °C, and the source ion temperature was 200 °C. The solvent cut time was set to 2.5, and the detector gain was set to relative mode with a threshold of 2000. Mass spectral data were recorded in scan mode, over the mass range, m/z 30-700, at a scan speed of 666-1428amu/s and event time 0.5 s. The identification of the chromatographic peaks was performed by comparing their mass spectra with those in the National Institute of Standards and Technology (NIST 05) library.

Molecular Docking Study

Protein-ligand interactions were studied with the help of PyRx by means of molecular docking simulations. PyRx is an online screening system that uses a combination of AutoDock Vina and AutoDock 4.2 (Lawal *et al.*, 2025). The PubChem database (www.pubchem.com) was used to retrieve phytochemical compounds and three FDA-approved reference drugs in SDF format. These were converted to the pdbqt format for docking studies (Lawal *et al.*, 2020; Gulati *et al.*, 2023). Three bacterial enzymes, enoyl-acyl carrier protein reductase (ECPR), UDP-N-acetylglucosamine enolpyruvyl transferase (MurA) and penicillin-binding protein (PBP) were selected as targets because they are essential metabolically and biosynthetically. Each enzyme had its own standard ligand for validation: Triclosan (PDB ID: 1D8A) for ECPR, Fospomycin (PDB ID: 3RK6) for MurA, and Amoxicillin (PDB ID: 3ITA) for PBP. These standards have been chosen as references to assess the affinities of the phytochemicals in the binding part, and they indicate their experimentally confirmed inhibitory potential.

Three-dimensional structures of the target proteins were downloaded from the Protein Data Bank (http://www.rcsb.org/pdb). The grid box analysis was used to identify active sites, focusing on the essential residues involved in ligand binding (Verma *et al.*, 2023). Protein structures were optimized by eliminating unnecessary water molecules. Geometric optimization was performed to obtain appropriate docking conformations. Simulations of docking were performed in PyRx, and ligands were docked into predicted active sites, and binding affinities were obtained. The resulting protein-ligand interactions (hydrogen bonds, hydrophobic contacts, and other force stabilizers) were examined with the help of PyMOL and the Protein-Ligand Interaction Profiler (PLIP) to gain a better understanding of the

binding modes and the effectiveness of the inhibitors (Spackman *et al.*, 2021; Verma *et al.*, 2022; Kumar *et al.*, 2024).

ADME Properties and Toxicity Prediction

The physicochemical properties, lipophilicity, water solubility, pharmacokinetics, drug-likeness and toxicity prediction, including the violation of Lipinski rule of five (Lipinski *et al.*, 1997) was studied using SwissADME online (http://www.swissadme.ch) (Lawal *et al.*, 2020) and ProTox-3.0 online software (https://tox.charite.de/protox3/index.php?site) (Banerjee *et al.*, 2024).

Data Analysis

The results of the conducted experiments were tabulated and summarised using descriptive statistics. The antibacterial activity was determined by measuring the inhibition zone diameter (mm) in three replicates and calculating the mean. Their direct comparison with ciprofloxacin results was used to determine the antibacterial activity of the extracts. To perform molecular characterization, sequence data from fungal isolates were compared using BLAST on the NCBI database to identify the species. The mass spectra of the compounds in the extracts were compared with those reported in the NIST library to identify them. The molecular docking results were evaluated based on binding affinity scores (kcal/mol) and interaction profiles. SwissADME and ProTox-3.0 predictions were used to determine pharmacokinetic and toxicological characteristics of the identified compounds. Tables, figures and descriptive summaries were used to state all interpreted data to facilitate comparative and inferential discussions.

RESULTS

Table 1: Identification of Endophytic Fungal Species Isolated from *Moringa oleifera*

Observed phenotypic characteristics of the isolate		Identified specie name	Reference(s) applied to identify the species name of the isolates
Macroscopy	Microscopy		
Downy white to yellow umbonate colonies with dark brown to black pinpoints and white border, with milk to a pale-yellow reverse side	Branched septate hyaline hyphae with long smooth conidiophores bearing large globose vesicles surrounded by radiate biseriate phialides	*Aspergillus niger*	Salisu *et al.* (2024a; 2022b)

Figure 1a: Macroscopic Features of *Aspergillus niger* Strain MOR-1

A description of both macroscopic and microscopic features of the isolated endophytic fungus was provided before molecular confirmation. The macroscopic features observed were downy white to yellow umbonate colonies with dark brown to black pinpoints and a white border, with a milk to pale-yellow reverse side (Figure 1a). Microscopically, the fungus exhibited branched, septate, hyaline hyphae with long, smooth conidiophores bearing large, globose vesicles surrounded by radiate, biseriate phialides (Figure 1b). These observed features were compared with those of already-identified fungal species to assess similarity. The macroscopic and microscopic features of the identified fungal species are also presented in Table 1.

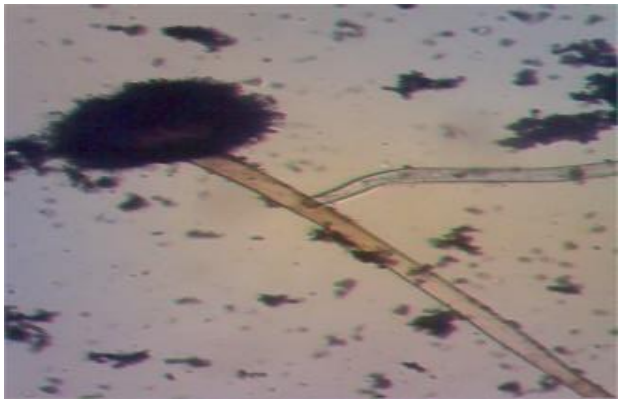

Figure 1b: Microscopic Features of *Aspergillus niger* Strain MOR-1

The molecular identification of the fungal organism was performed by blasting the sequenced nucleotides of the ITS1 and ITS4 regions against the NCBI database. The query sequence corresponded to the *Aspergillus niger* strain LA01, namely the 5.8S ribosomal RNA gene and the internal transcribed spacer 2 (ITS2), complete sequence; and the 28S ribosomal RNA gene, partial sequence (GenBank accession number: HQ392475.1). The percentage of similarity was 100. The phylogenetic tree generated using the maximum likelihood technique against ITS sequences of already known fungal species is illustrated in Table 2 and Figure 2, and the outcome affirmed the fungal organism to be related to the *Aspergillus niger* strain HQ392475.1

Table 2: Molecular Identification of Endophytic Fungi Using BLASTn Search

Isolate's DNA Sequence	Identified Species	BLASTn Search Matched Species	% Similarity
TGCGGAAGGATCATTACCGAGTGCGGGTCCTTTGG GCCCAACCTCCCATCCGTGTCTATTGTACCCTGTTG CTTCGGCGGGCCCGCCGCTTGTCGGCCGCCGGGG GGGCGCCTCTGCCCCCCGGGCCCGTGCCCGCCGGA GACCCCAACACGAACACTGTCTGAAAGCGTGCAGT CTGAGTTGATTGAATGCAATCAGTTAAAACTTTCAA CAATGGATCTCTTGGTTCCGGCATCGATGAAGAAC GCAGCGAAATGCGATAACTAATGTGAATTGCAGAA TTCAGTGAATCATCGAGTCTTTGAACGCACATTGCG CCCCCTGGTATTCCGGGGGGCATGCCTGTCCGAGC GTCATTGCTGCCCTCAAGCCCGGCTTGTGTGTTGG GTCGCCGTCCCCCTCTCCGGGGGGGACGGGCCCGAA AGGCAGCGGCGGCACCGCGTCCGATCCTCGAGCGT ATGGGGCTTTGTCACATGCTCTGTAGGATTGGCCG GCGCCTGCCGACGTTTTCCAACCATTCTTTCCAGGT TGACCTCGGATCAGGTAGGGATACCCGCTGAACTT AAGCATATCAATAAGCGGAGGAA	*Aspergillus niger*	HQ392475.1 *Aspergillus niger* strain LA01	100.00
		KJ410675.1 *Aspergillus niger* PSF-5	100.00
		MZ376739.1 *Aspergillus niger* Strain WJ-1	100.00
		LC573605.1 *Aspergillus niger* NBRC:6661	100.00
		HQ014692.1 ***A****spergillus niger* strain WM10.70	100.00

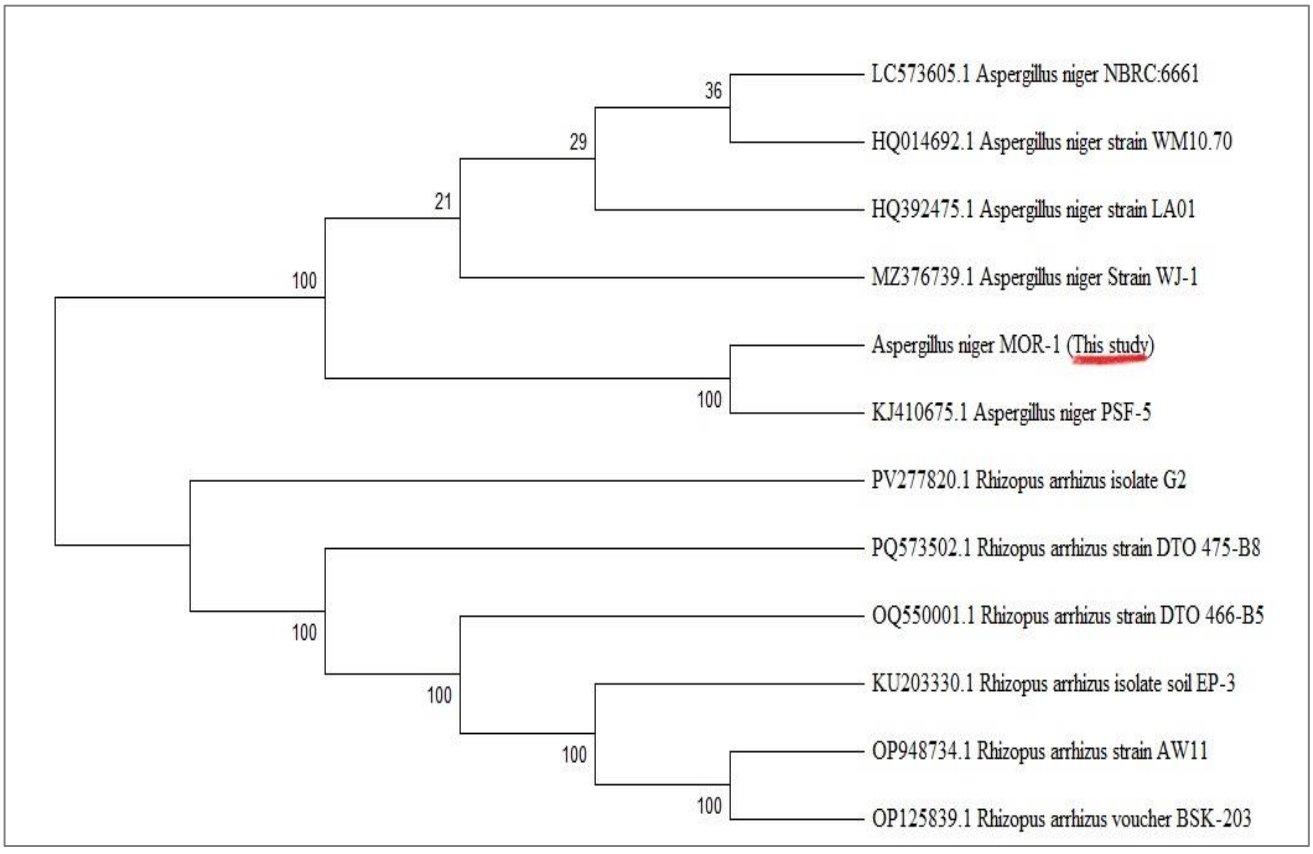

Figure 2: Neighbour-Joining tree showing the evolutionary relationship between *Aspergillus niger* MOR-1 from this study and other similar isolates from NCBI GenBank

Antibacterial activity of the crude extract of the identified endophytic fungal isolate was measured as the mean zone of inhibition (mm) against the pathogenic bacterial strains (Table 3). *Aspergillus niger* MOR-1 appears to be widespread and a very effective antibacterial candidate, with the ability to produce an inhibition zone similar to that of ciprofloxacin against various pathogens. It inhibited *S. aureus* and *S. pneumoniae* with 21.67 ± 1.53 mm and 20.33 ± 1.53 mm zones of inhibition, respectively; slightly higher than the 20.6 ± 0.29 mm and notably lower than the 28.8 ± 0.38 mm zones recorded by the control for the respective bacteria. Yet it showed no effect on MRSA, which, interestingly, aligns with the inactivity observed in the control. More strikingly, it exhibited activity against *P. aeruginosa* (16.67 ± 1.53 mm) higher than the 12.10 ± 1.05 mm inhibition by the control, and activity on three *Enterobacteriaceae*: *K. pneumoniae* (29.33 ± 1.53 mm), *S. typhii* (29.33 ± 2.52 mm), and *E. coli* (28.33 ± 1.53 mm) all substantially higher than the

control's 24.6 ± 0.23 mm, 27.00 ± 1.00 mm, and 25.5 ± 0.47 mm respectively. The lack of inhibition of Shigella spp., Citrobacter spp., and Bacillus sp. hints at target-specific resistance traits, whereas the control exhibited substantial zones of 28.8 ± 0.38 mm, no activity, and 30.1 ± 0.41 mm, respectively, against these isolates.

Table 3: Antibacterial Activity of Crude Extract of *Aspergillus niger* MOR-1

Extract/ Control	Zone of Inhibition (Mean ± SD mm)									
	S. aureus	*P. aeruginosa*	*K. pneumonia*	*MRSA*	*S. pneumonia*	*S. typhii*	*Shigella sp.*	*Citrobacter*	*Bacillus sp.*	*E. coli*
M	21.67 ± 1.53	16.67 ± 1.53	29.33 ± 1.53	-	20.33 ± 1.53	9.33 ± 2.52	-	-	-	28.33 ± 1.53
C	20.6 ± 0.29	12.10 ± 1.05	24.6 ± 0.23	-	28.8 ± 0.38	7.00 ± 1.00	28.8 ± 0.38	-	30.1 ± 0.41	25.5 ± 0.47

KEY: M: MOR-1; C Ciprofloxacin

Table 4: GCMS Result of Crude Extract of *Aspergillus niger* strain MOR-1

PN	Area (%)	Comp. CID	IUPAC Name	MW (g/mol)	Molecular Formula	Chemical Structure
1	11.87	14259	Methyl eicosanoate	326	$C_{21}H_{42}O_2$	
2	46.66	21205	Methyl 14-methylpentadecanoate	270	$C_{17}H_{34}O_2$	
3	25.17	5354133	Methyl ricinoleate	312	$C_{19}H_{36}O_3$	
4	4.56	5362793	Methyl (13E,16E)-13,16-octadecadienoate	294	$C_{19}H_{34}O_2$	
5	1.44	5362805	Methyl (6E,9E,12E)-6,9,12-octadecatrienoate	292	$C_{19}H_{32}O_2$	
6	1.77	6421258	Arachidonic acid methyl ester		$C_{21}H_{34}O_2$	
7	0.89	5364432	Methyl (11E)-11-octadecenoate	296	$C_{19}H_{36}O_2$	
8	0.53	5365682	9,12-Octadecadien-1-ol, (Z,Z)-	266	$C_{18}H_{34}O$	
9	7.11	8201	Methyl n-octadecanoate	298	$C_{19}H_{38}O_2$	

KEY: PN: Pk Number; Comp. CID: Compound CID; MW: Molecular Weight

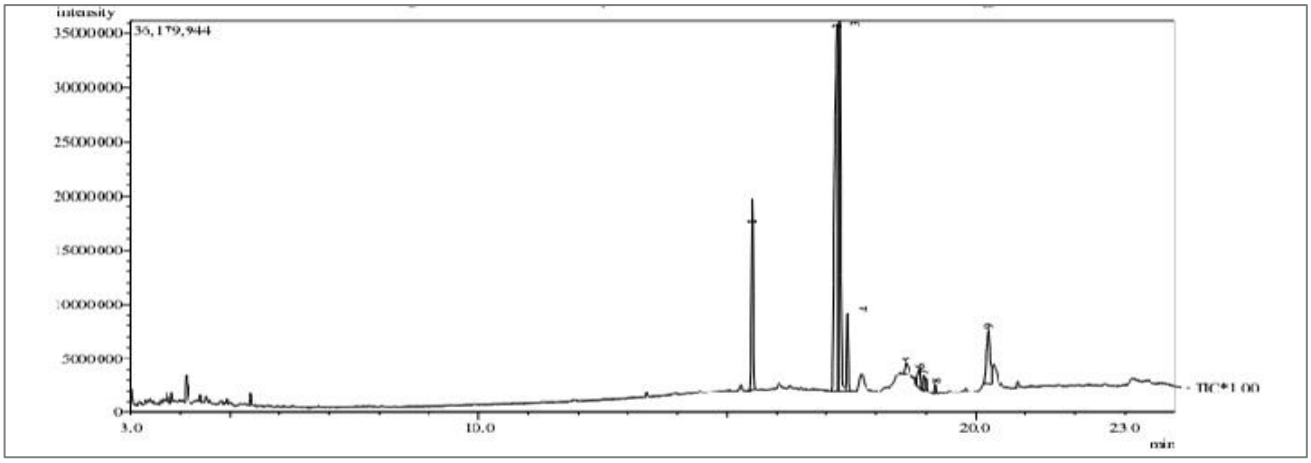

Figure 3: GC-MS Chromatogram of *Aspergillus niger* strain MOR-1

Analysis of crude extract of *Aspergillus niger* MOR-1 using Gas Chromatography-Mass Spectrometry (GC-MS) demonstrated various fatty acid methyl esters (FAMEs) and lipid derivatives to be the primary components of the fungi metabolic profile (Table 4 & Fig. 3). The chromatogram exhibited a number of peaks that represented structurally different aliphatic substances with molecular weights of between 266 and 326 g/mol. The range shows that long-chain fatty acid esters and unsaturated lipid molecules are preponderant. The data indicate that methyl eicosanoate (11.87%), methyl 14-methylpentadecanoate (46.66%), methyl ricinoleate (25.17%), methyl (13E,16E)-13,16-octadecadienoate (4.56%), methyl (6E,9E,12E)-6,9,12-octadecatrienoate (1.44%), arachidonic acid methyl.

Table 5: FTIR Result of Crude Extract of Aspergillus niger MOR-1

Peak (cm^{-1})	Intensity	Functional Group	Compound Class	Reference(s) used to identify the compound class
867.03	91.344	=C–H bending	Alkene	Nassar *et al.* (2023); Salisu *et al.*, (2022)
1071.49	90.404	C–O stretching	Aliphatic ether	Nongthombam *et al.* (2024); Gupta *et al.* (2025)
1230.63	91.054	C–N stretching	Aliphatic amine	Gupta *et al.* (2025)
1406.15	90.784	CH2 bending	Lipid/Protein	Wittayapipath *et al.* (2019)
1523.82	89.786	N–O stretching	Nitro compound	Niazi *et al.* (2023); Salisu *et al.*, (2020)
1633.76	90.217	C=O stretching	Amide	Pramitha *et al.* (2021)
1761.07	92.025	C=O stretching	Ketone	Nongthombam *et al.* (2024)
2342.62	91.418	O=C=O stretching	Carbon dioxide	Osunde *et al.* (2024)
2633.89	91.244	O–H stretching	Alcohol	Nongthombam *et al.* (2024); Gupta *et al.* (2025)
2820.02	90.938	C–H stretching	Aldehyde	Muthukrishnan *et al.* (2022)
2820.02	90.938	C–H stretching	Aldehyde	Muthukrishnan *et al.* (2022)
2885.6	91.049	–CH2– stretching	Fatty acid	Nikolova *et al.* (2025)
3074.63	90.448	=C–H stretching	Alkene	Nassar *et al.* (2023)
3140.22	90.409	N–H stretching	Amine	Maliehe *et al.* (2022); Nongthombam *et al.* (2024)
3218.34	90.26	N–H stretching	Amine	Maliehe *et al.* (2022); Nongthombam *et al.* (2024)
3298.38	90.534	O–H stretching	Alcohol	Nongthombam *et al.* (2024); Gupta *et al.* (2025)
3443.05	90.693	O–H stretching	Alcohol	Nongthombam *et al.* (2024); Gupta *et al.* (2025)
3625.33	89.665	O–H stretching	Alcohol	Nongthombam *et al.* (2024); Gupta *et al.* (2025)
3741.06	89.543	O–H stretching	Alcohol	Nongthombam *et al.* (2024); Gupta *et al.* (2025)
3810.5	89.339	O–H stretching	Alcohol	Nongthombam *et al.* (2024); Gupta *et al.* (2025)
3855.83	89.217	O–H stretching	Alcohol	Nongthombam *et al.* (2024); Gupta *et al.* (2025)
3934.92	89.401	N–H stretching	Amine	Maliehe *et al.* (2022); Nongthombam *et al.* (2024)

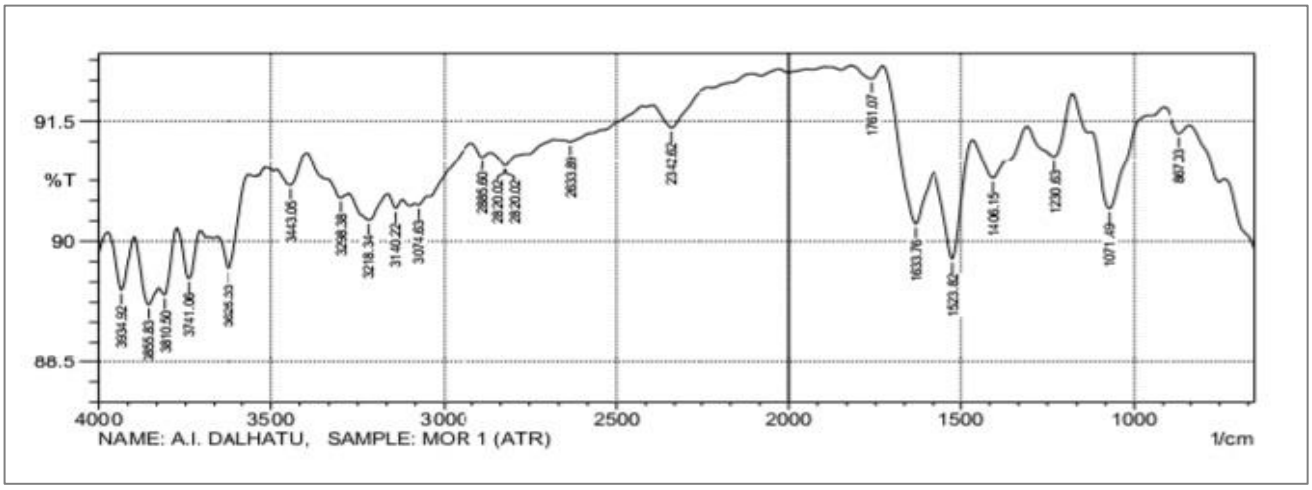

Figure 4: FTIR – Chromatogram of *Aspergillus niger* strain MOR-1

Table 6: Molecular Docking Result of Bioactive Compounds from Crude Extract of *Aspergillus niger* (MOR-1) Against Bacterial Target Proteins

	Target proteins (PDB ID)			Reference used in selecting standard
Compound CID:	***ECPR (1D7O)***	**MurA *(1A2N)***	**PBPs (*2BG1*)**	
14259	***-5.6***	***-5.8***	***-5.9***	
21205	*-5.7*	*-5.6*	*-4.9*	
5354133	***-6.0***	***-5.7***	***-6.2***	
5362793	*-5.5*	*-5.4*	*-5.3*	
5362805	***-5.6***	***-5.5***	***-5.8***	
6421258	*-5.3*	*-5.5*	*-4.0*	
5364432	*-5.6*	*-5.4*	*-5.8*	
5365682	*-5.6*	*-5.7*	*-5.0*	
8201	*-5.6*	*-5.5*	*-5.2*	
Triclosan (1D8A)	*-5.2*	-----	-----	Katiki *et al.* (2022)
Fosfomycin (3RK6)	-----	*-4.7*	-----	Amrutha *et al.* (2025)
Amoxicillin (3ITA)	-----	-----	*-4.8*	Attaran *et al.* (2021)

Table 7: Amino Acid Interaction Profiles of Selected Bioactive Compounds from Crude Extract of *Aspergillus niger* strain MOR-1 with Bacterial Target Proteins

Protein	Compound ID	Binding affinities (kcal/mol)	Ligand-AA Residues	
			H-bond	Hydrophobic interactions
ECPR (1D7O)	14259	-5.6	---------	ASN30A, TRP52A, ILE247A
	5354133	-6.0	--------	ILE247A, ILE251A.
	5362805	-5.6	--------	ILE247A
MurA (1A2N)	14259	-5.8	--------	ARG91A, ALA115A, ARG120A, VAL122A, ASP369A
	5354133	-5.7	GLY114A, LEU370A	ARG91A, LUE111A, ARG120A, VAL122A, ASP369A.
	5362805	-5.5	------	ARG91A, ALA115A, ARG120A, ASP369A
PBPs (2BG1)	14259	-5.9	GLU346A	GLN582A, LYS583A.
	5354133	-6.2	TYR580A, GLN582A, LYS583A.	PHE452A, LYS583A,
	5362805	-5.8	LYS583A.	GLU545A, GLN582A, LYS583A.

Table 8: Drug-likeness, Lipophilicity, and Physicochemical Properties of Selected Bioactive Compounds from Crude Extract of *Aspergillus niger* strain MOR-1

Compound ID	MW (g/mol)	TPSA	n-HBD	n-HBA	n-ROTB	M Ref	Log P	L.V	Pre. (mg/kg)	LD_{50}
CID14259	326.56	26.30	0	2	19	104.35	7.20	1	5000	
CID5354133	312.49	46.53	1	3	16	95.42	5.17	1	3000	
CID5362805	292.46	26.30	0	2	14	93.31	5.75	1	20000	
Standard	≤ 500	≤ 140	≤ 5	≤ 10	≤ 10	40–230	≤ 5	---	> 2000	

Table 9: Toxicity Prediction of *Selected Bioactive Compounds* from Crude Extract of *Aspergillus niger* strain MOR-1

Compound CID	Acute oral toxicity	Blood-Brain Barrier	Nutritional toxicity	Carcinogenicity	Hepatotoxicity	Nephrotoxicity	Neurotoxicity	GI- Absorption	Human Oral Bioavailability	p-glycoprotein inhibitor	CYP1A2-inhibitor	CYP2C19 inhibitor	CYP2C9 inhibitor	CYP2D6 inhibitor	CYP3A4 inhibitor	CYP2E1 inhibitor
14259	Class V	+	-	-	-	-	-	+	-	+	-	-	-	-	-	-
5354133	Class V	+	-	-	-	-	-	+	-	+	-	-	-	-	-	-
5362805	Class VI	+	-	-	-	-	-	+	-	-	+	-	+	-	-	-

The FTIR spectrum of the crude extract of *Aspergillus niger* strain MOR-1 (Table 5 & Fig. 4) showed that it had a wide range of functional groups that were characteristic of its complicated biochemical structure. =C-H bending at 867.03 cm^{-1} and =C-H stretching at 3074.63 cm^{-1} was used to identify alkenes, and C-O and C-N stretching at 1071.49 cm^{-1} and 1230.63 cm^{-1}, respectively, were used to identify ethers and amines. The CH2 bending at 1406.15 cm^{-1} and CH2 stretching at 2885.60 cm^{-1} indicated lipid or fatty acids, and the C-H stretching at 2820.02 cm^{-1} indicated aldehydes. Nitro compounds were identified by N-O at 1523.82 cm^{-1}, proteinaceous or nitrogenous metabolites by amide C=O at 1633.76 cm^{-1}, and ketones by C=O at 1761.07 cm^{-1}. The O=C=O band detected the presence of carbon dioxide at 2342.62 cm^{-1}, and, at the same time, the presence of alcohols and hydroxyl groups was detected by the O-H band at 2633.89 cm^{-1} and by an extensive range of other peaks at 3298.38-3855.83 cm^{-1}. Moreover, N-H amines were detected at 3140.22, 3218.34, and 3934.92 cm^{-1}, which, together, confirmed the presence of diverse biochemical components in the fungal extract.

Molecular docking of the identified bioactive compounds in the crude extract of *Aspergillus niger* MOR-1 was performed to analyse their potential inhibitory effects on the bacterial essential enzymes ECPR, MurA, and PBPs. Table 6 shows that the docking scores of the studied compounds ranged from -4.0 to -6.2 kcal/mol, indicating that the fungal metabolites have favourable binding affinities for the active sites of the target proteins. The fungal compounds had greater or similar affinities when compared to the docking scores of the standards, ECPR (Triclosan (-5.2 kcal/mol)), MurA (Fosfomycin (-4.7 kcal/mol)) and PBPs (Amoxicillin (-4.8 kcal/mol)), indicating that the compounds hold promise in inhibitory ability.

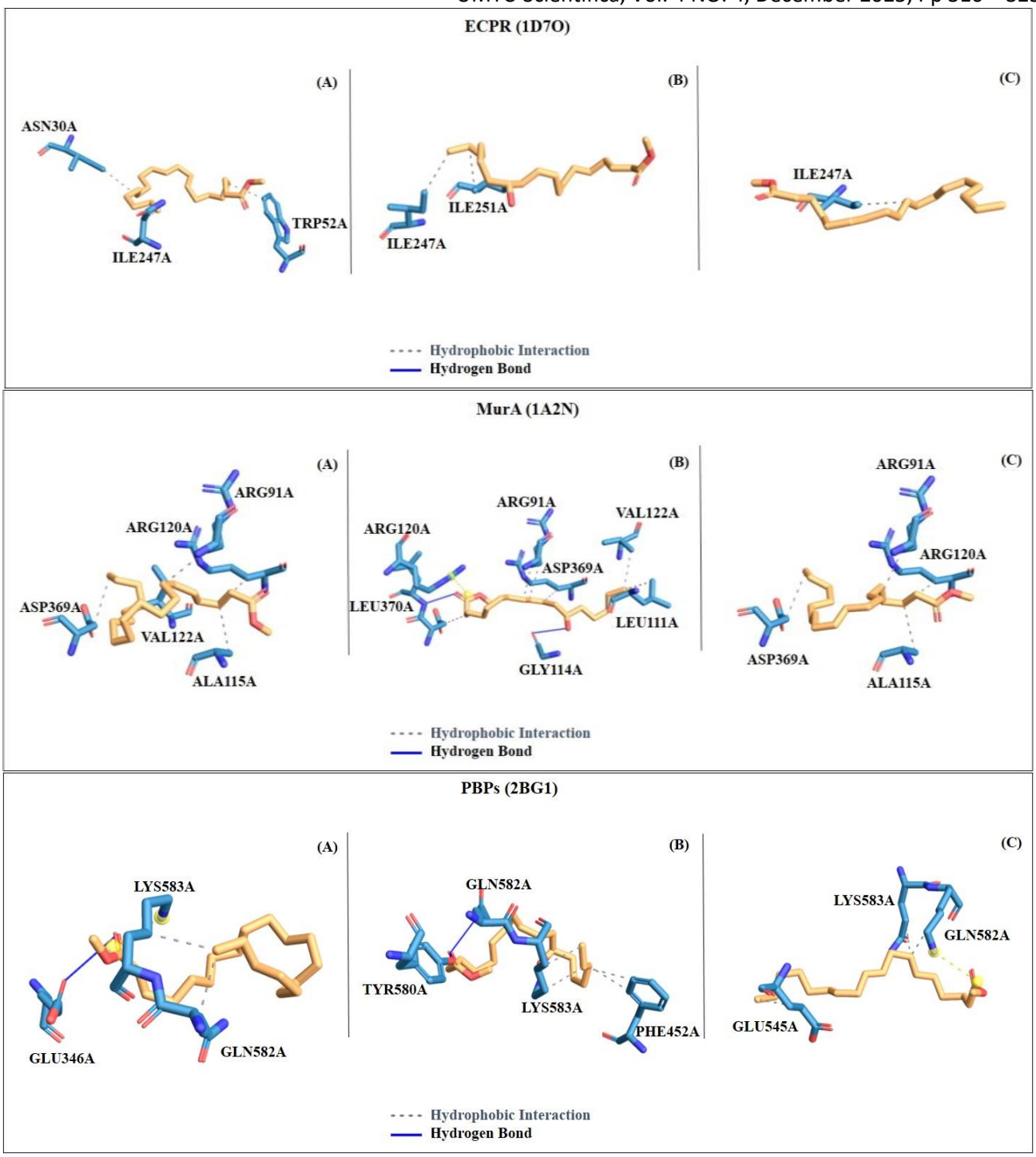

Figure 5: 3D docking pose interactions of ECPR, MurA and PBPs target proteins with bioactive compounds: (A) CID14259, (B) CID5354133, and (C) CID5362805 derived from *extracts of Aspergillus niger strain MOR-1*

The most promising compound screened was methyl ricinoleate (CID 5354133), with the highest binding affinities with all targets (-6.0, -5.7, and -6.2 kcal/mol, respectively). Other compounds, including methyl (6E,9E,12E)-6,9,12-octadecatrienoate (CID 5362805) and methyl (11E)-11-octadecenoate (CID 5364432), were also found to have significant binding affinity, especially to PBPs and ECPR. The general docking trend shows that the fungal metabolites, which are mainly long-chain fatty acid esters and unsaturated lipids, have high affinity for bacterial enzymatic targets, increasing their promise as a potential source of natural antibacterial activity (Figure 5).

Interaction analysis of selected bioactive compounds in the crude extract of *Aspergillus niger* MOR-1 with three major bacterial target enzymes, as illustrated in Table 7, reveals that the compounds exhibit strong binding affinities for the active-site residues of the target proteins. In the ECPR, the primary interactions involve residues ASN30A, TRP52A, ILE247A, and ILE251A. The ligands of MurA interacted with ARG91A, ALA115A, ARG120A, and ASP369A. It also forms hydrogen bonds with GLY114A and LEU370A, demonstrating stable, specific binding in the MurA active pocket. In the case of PBPs, several hydrogen bonds and hydrophobic

interactions with key residues, including TYR580A, GLN582A, GLU545A, and LYS583A, are observed in their interaction profiles.

[a] MW: molecular weight (<500, expressed as Dalton); [b] TPSA: Topological polar surface area (≤ 140 Å²); [c] n-HBD: number of hydrogen bond donors (≤5); [d] n-HBA: number of hydrogen bond acceptors (≤10); [e] n-ROTB: number of rotatable bonds (≤ 10); [f] M Ref: molar refractivity (40–230); [f] LogP: logarithm of partition coefficient (<5) of compound between n-octanol and water; [g] LV: Lipinski's violation; [i] Pre. LD50: Predicted LD50 (> 2000) (Nhlapho *et al.*, 2024).

The data in Table 8 show the estimated drug-likeness, lipophilicity, and physicochemical key parameters of the active compounds identified in crude extracts of the *Aspergillus niger* strain MOR-1. Key parameters include molecular weight, topological polar surface area (TPSA), hydrogen bond donors and acceptors, rotatable bonds, molar refractivity, Log P, Lipinski violations, and predicted median lethal dose (LD_{50}). The compounds displayed molecular weights of 292.46–326.56 g/mol and TPSA values of 26.30–46.53 Å². Hydrogen bond donors ranged from 0–1, acceptors from 2–3, and rotatable bonds from 14–19. Log P values ranged from 5.17 to 7.20, and each compound exhibited one Lipinski violation. Predicted LD_{50} values ranged from 48 to 20,000 mg/kg. Reference threshold values for standard drug-likeness parameters are provided for comparison

The data in Table 9 present the in-silico toxicity profiles of selected bioactive compounds from *Aspergillus niger* (MOR-1). The parameters include acute oral toxicity class, blood–brain barrier (BBB) permeability, gastrointestinal absorption, nutritional toxicity, carcinogenicity, hepatotoxicity, nephrotoxicity, neurotoxicity, human oral bioavailability, P-glycoprotein inhibition, and cytochrome P450 (CYP) isoform inhibition.

The predicted acute oral toxicity of the identified compounds ranged between Class V and Class VI, indicating low acute toxicity. All compounds demonstrated positive blood–brain barrier permeability and high gastrointestinal absorption, while none showed predicted nutritional toxicity, carcinogenicity, hepatotoxicity, nephrotoxicity, or neurotoxicity. Human oral bioavailability was predicted to be negative for all compounds. With respect to metabolic interactions, two compounds (CIDs 14259 and 5354133) were predicted to inhibit P-glycoprotein, whereas CID 5362805 showed no P-glycoprotein inhibitory activity. Limited cytochrome P450 inhibition was observed, with CID 5362805 predicted to inhibit CYP1A2 and CYP2C19, while no inhibitory effects were predicted for CYP2C9, CYP2D6, CYP3A4, or CYP2E1 across all compounds.

DISCUSSION

Moringa oleifera offers a chemically diverse platform on which endophytic fungi with potential antibacterial activity can be selected and characterized. Particular attention is given to leaves for both practical and scientific reasons, such as their primary role in secondary metabolism and their value as hosts for microbial symbionts (Pang *et al.*, 2021). Recent phytochemical and microbiological data are supported by the plant's ethnopharmacological history and thus confirm the hypothesis that its endophytes could produce new bioactive substances. Therefore, the host plant is scientifically justified as a potential source for bioprospecting and the identification of natural products, consistent with its traditional use as medicine.

Following isolation, antibacterial screening against ten clinical bacterial isolates revealed detectable inhibitory activity, highlighting the selective nature of antibacterial metabolite production by the endophytic fungi. Zones of inhibition were quantified as mean ± SD, and comparative analysis against a standard antibiotic control provided a framework for assessing relative potency, spectrum, and limitations. The observed variability in antibacterial activity reflects differences in fungal secondary metabolite composition and in bacterial structural defences, including outer membrane permeability and intrinsic resistance mechanisms.

Within this context, *Aspergillus niger* strain (MOR-1) exhibited a broad and potent antibacterial spectrum. Inhibition against *S. aureus* and *S. pneumoniae* was comparable to the control. Notably, MOR-1 demonstrated activity against *P. aeruginosa*, *K. pneumoniae*, *S. typhi*, and *E. coli*, exceeding control values in each case. The lack of activity against MRSA and certain enteric species suggests the presence of strain-specific resistance mechanisms. The activity against *S. pneumoniae* aligns closely with the findings of Baz *et al.* (2024), who reported an inhibition zone of 18 ± 0.11 mm for *A. niger* culture filtrate extract. Notably, the activity against *S. aureus* observed in this study is more than double the 10.5 ± 0.08 mm inhibition reported by Baz *et al.* (2024), underscoring the extract's greater potency. The inhibition zone on *E. coli* exceeds the 23.5 ± 0.06 mm observed by Baz *et al.* (2024), indicating a stronger antibacterial effect.

The inhibition of *S. aureus* concurs with the 15.66 ± 0.57 mm (Rani *et al.*, 2017), 18.39 ± 0.03 mm (Niazi *et al.*, 2023), and 10.157 ± 0.79 mm (Satriawan *et al.*, 2025) reports, but contradicts the total inactivity noted by Fuego *et al.* (2021). Similarly, the absence of MRSA activity conflicts with Satriawan *et al.* (2025) (12.57 ± 1.09 mm). The *P. aeruginosa* zone aligns with Enany *et al.* (2022) (16.5 ± 0.71 mm) and Ramesh *et al.* (2022) (19.33 mm), and is virtually identical to the 17.0 ± 0.18 mm of Baz *et al.* (2024), yet surpasses the 3.8 ± 0.8 mm reported by Ababutain *et al.* (2021). The activity against *K. pneumoniae* and *S. typhii* is consistent with earlier reports (Rani *et al.*, 2017; Khattak *et al.*, 2021; Ramesh *et al.*, 2022) but markedly exceeds the diameters reported by Ababutain *et al.* (2021) and Niazi *et al.* (2023). Finally, the lack of activity against *Bacillus* spp. contrasts with the 22.35 ± 0.20 mm inhibition of *B. subtilis* found by Niazi *et al.* (2023) and the activity recorded by Fuego *et al.* (2021). The exceptional potency of MOR-1 likely arises from a synergistic mixture of low-molecular-weight

polyketides and ionophore-like compounds capable of disrupting proton gradients and membrane integrity (Rani *et al.*, 2021; Liu *et al.*, 2025).

In support of this observation, FTIR and GC–MS results indicated a lipid-centric profile, suggesting the abundance of hydroxylated and unsaturated fatty acid esters. These amphiphilic molecules can integrate into bacterial membranes, induce oxidative stress, and impair enzymatic function (Harayama and Antonny, 2023; Trabelsi *et al.*, 2023; Jomova *et al.*, 2023). The convergence of spectroscopic and chromatographic data supports the extract's pronounced antibacterial efficacy and ecological fitness.

At the molecular level, docking analysis revealed favourable binding of selected compounds to ECPR, MurA, and PBPs, enzymes essential for bacterial lipid synthesis and cell wall integrity. Compounds from *A. niger* strain MOR-1 consistently exhibited strong affinities (up to −6.2 kcal/mol), likely due to optimal hydrophobic complementarity within enzyme pockets (Abdellatief *et al.*, 2025; Alanazi, 2025). Protein–ligand interactions were stabilized by hydrogen bonding and hydrophobic contacts involving catalytically relevant residues, thereby validating the docking predictions.

Furthermore, ADME/T profiling indicated that all selected compounds comply with Lipinski's rule of five and exhibit favorable pharmacokinetic properties. Most compounds belonged to low-toxicity classes (V–VI), with minimal CYP450 and P-gp inhibition, suggesting a low risk of drug–drug interactions and efflux-mediated resistance (Cheng *et al.*, 2012). Collectively, these attributes support their candidacy for further preclinical development.

CONCLUSION

Moringa oleifera leaves provide a scientifically validated platform for screening for antibacterial endophytic fungi. The endophytic strain *Aspergillus niger* MOR-1 demonstrated broad and significant antibacterial activity against various clinically relevant pathogens, often equaling or surpassing standard antibiotic treatments, though with specific limitations across strains. Analyses using spectroscopy and chromatography indicated a metabolite profile high in lipids, primarily consisting of amphiphilic fatty acid derivatives, which support membrane-disruptive antibacterial mechanisms. Molecular docking studies revealed strong, stable interactions between selected compounds and key bacterial enzymes, while ADME/T predictions indicated favourable drug-like properties and minimal toxicity. Altogether, these observations position *A. niger* strain MOR-1 as a potential source of new antibacterial agents and encourage further purification and preclinical investigation.

REFERENCES

Ababutain, I. M., Aldosary, S. K., Aljuraifani, A. A., Alghamdi, A. I., Alabdalall, A. H., Al-Khaldi, E. M., & Borgio, J. F. (2021). Identification and antibacterial characterization of endophytic fungi from *Artemisia sieberi*. *International Journal of Microbiology, 2021*(1), 6651020. [Crossref]

Abdelalatif, A. M., Elwakil, B. H., Mohamed, M. Z., Hagar, M., & Olama, Z. A. (2023). Fungal secondary metabolites/dicationic pyridinium iodide combinations in combat against multi-drug resistant microorganisms. *Molecules, 28*(6), 2434. [Crossref]

Abdelaziz, A. M., Hashem, A. H., Abd-Elsalam, K. A., & Attia, M. S. (2025). Biodiversity of fungal endophytes. In *Fungal endophytes volume I: Biodiversity and bioactive materials* (pp. 43–61). Springer Nature Singapore. [Crossref]

Abdelgawad, M. A., Hamed, A. A., Nayl, A. A., Badawy, M. S. E., Ghoneim, M. M., Sayed, A. M., & Gamaleldin, N. M. (2022). The chemical profiling, docking study, and antimicrobial and antibiofilm activities of the endophytic fungi *Aspergillus* sp. AP5. *Molecules, 27*(5), 1704. [Crossref]

Adeleke, B. S., & Babalola, O. O. (2021). Pharmacological potential of fungal endophytes associated with medicinal plants: A review. *Journal of Fungi, 7*(2), 147. [Crossref]

Aghdam, S. A., & Brown, A. M. V. (2021). Deep learning approaches for natural product discovery from plant endophytic microbiomes. *Environmental Microbiome, 16*(1), 6. [Crossref]

Alanazi, Y. N. (2025). *Role of penicillin binding proteins in synthesis and modification of bacterial cell envelope* [Doctoral dissertation, Newcastle University]. [Link]

Amrutha, S., Das, P., Nayak, A., Laha, S., Begum, S., & Bhardwaj, S. (2025). Synthesis and anti-microbial evaluation with in silico studies of novel 2-aminothiazole benzohydrazide derivatives. *Future Journal of Pharmaceutical Sciences, 11*(1), 6. [Crossref]

Attaran, B., Salehi, N., Ghadiri, B., Esmaeili, M., Kalateh, S., Tashakoripour, M., & Mohammadi, M. (2021). The penicillin binding protein 1A of *Helicobacter pylori*, its amoxicillin binding site and access routes. *Gut Pathogens, 13*(1), 43. [Crossref]

Bala, K., Joshi, S., Brar, B., Berwal, A., Banger, S. P., & Budania, L. S. (2025). Diversity and functional role of fungal endophytes. In *Metabolic sustainability of endophytes: Current status, challenges and potential* (pp. 13–35). Springer Nature Singapore. [Crossref]

Banerjee, P., Kemmler, E., Dunkel, M., & Preissner, R. (2024). ProTox 3.0: A webserver for the prediction of toxicity of chemicals. *Nucleic Acids Research, 52*(W1), W513–W520. [Crossref]

Baz, A. M., Elwy, E., Ahmed, W. A., & El-Sayed, H. (2024). Metabolic profiling, antimicrobial, anticancer, and in vitro and in silico immunomodulatory investigation of *Aspergillus niger* OR730979 isolated from the Western Desert, Egypt. *International Microbiology*, 1–15. [Crossref]

Bielecka, M., Pencakowski, B., & Nicoletti, R. (2022). Using next-generation sequencing technology to

explore genetic pathways in endophytic fungi in the syntheses of plant bioactive metabolites. *Agriculture, 12*(2), 187. [Crossref]

Buddhika, U. V. A., & Abeysinghe, S. (2020). Secondary metabolites from microbes for plant disease management. In *Emerging trends in plant pathology* (pp. 331–342). Springer Singapore. [Crossref]

Chakraborty, S., Debnath, D., Mahapatra, S., & Das, S. (2021). Role of endophytes in plant disease management. In *Emerging trends in plant pathology* (pp. 399–424). Springer. [Crossref]

Chandra, P., & Enespa. (2019). Soil-microbes-plants: Interactions and ecological diversity. In *Plant microbe interface* (pp. 145–176). Springer. [Crossref]

Cheng, F., Li, W., Zhou, Y., Shen, J., Wu, Z., Liu, G., Lee, P. W., & Tang, Y. (2012). admetSAR: A comprehensive source and free tool for assessment of chemical ADMET properties. *Journal of Chemical Information and Modeling, 52*(11), 3099–3105. [Crossref]

Dar, R. A., Shahnawaz, M., Ahanger, M. A., & Majid, I. U. (2023). Exploring the diverse bioactive compounds from medicinal plants: A review. *Journal of Phytopharmacology, 12*(3), 189–195. [Crossref]

Das, M., Kityania, S., Nath, R., Nath, R., Nath, D., & Talukdar, A. D. (2024). Endophytic fungi and the health benefits from their potential bioactive secondary metabolites. In *Endophytic fungi: The hidden sustainable jewels for the pharmaceutical and agricultural industries* (pp. 295–324). Springer International Publishing. [Crossref]

Elshobary, M. E., Badawy, N. K., Ashraf, Y., Zatioun, A. A., Masriya, H. H., Ammar, M. M., & Assy, A. M. (2025). Combating antibiotic resistance: Mechanisms, multidrug-resistant pathogens, and novel therapeutic approaches: An updated review. *Pharmaceuticals, 18*(3), 402. [Crossref]

Enany, M. E., Wahid, O. A. A., Salama, S. S. A. E. H., & Abd El-Salam, S. A. (2022). Antibacterial activity of bioactive compounds from endophytic fungi against *P. aeruginosa* isolated from freshwater fishes. *Egyptian Journal of Aquatic Biology and Fisheries, 26*, 469–490. [Crossref]

Eo, J. K., Choi, J. W., & Eom, A. H. (2022). Diversity, distribution, and host plant of endophytic fungi: A focus on Korea. *Mycobiology, 50*(6), 399–407. [Crossref]

Eshboev, F., Mamadalieva, N., Nazarov, P. A., Hussain, H., Katanaev, V., Egamberdieva, D., & Azimova, S. (2024). Antimicrobial action mechanisms of natural compounds isolated from endophytic microorganisms. *Antibiotics, 13*(3), 271. [Crossref]

Etanke, E. S., Besem, A. D., Afanga, A. Y., Joice, M., Bechem, E. T., & Ambo, F. B. (2021). Molecular identification of endophytic fungi associated with orchids from Mount Cameroon region. *African Journal of Biological Sciences, 3*(2), 95–106. [Crossref]

Fuego, B. N., Romano, K. G., Pinlac, C. D., & Lirio, G. A. C. (2021). Evaluation of the antimicrobial activity of endophytic fungus isolated from *Cocos nucifera* (L.) cotyledon against medically-important pathogens. *Journal of Biosciences and Medicines, 9*(1), 86–97. [Crossref]

Gakuubi, M. M., Munusamy, M., Liang, Z. X., & Ng, S. B. (2021). Fungal endophytes: A promising frontier for discovery of novel bioactive compounds. *Journal of Fungi, 7*(10), 786. [Crossref]

Grabka, R., d'Entremont, T. W., Adams, S. J., Walker, A. K., Tanney, J. B., Abbasi, P. A., & Ali, S. (2022). Fungal endophytes and their role in agricultural plant protection against pests and pathogens. *Plants, 11*(3), 384. [Crossref]

Gulati, P., Kumar Verma, A., Kumar, A., & Solanki, P. (2023). Para-cresyl sulfate and BSA conjugation for developing aptasensor: Spectroscopic methods and molecular simulation. *ECS Journal of Solid State Science and Technology, 12*(7), 073004. [Crossref]

Gupta, A., Pandey, B. C., Yaseen, M., Kushwaha, R., Shukla, M., Chaudhary, P., & Kumari, N. (2025). Exploring anticancer, antioxidant, and antimicrobial potential of *Aspergillus flavus*, a fungal endophyte isolated from *Dillenia indica* leaf callus. *Heliyon, 11*(3), Article e42142. [Crossref]

Harayama, T., & Antonny, B. (2023). Beyond fluidity: The role of lipid unsaturation in membrane function. *Cold Spring Harbor Perspectives in Biology, 15*(7), a041409. [Crossref]

Hur, J. Y., Jeong, E., Kim, Y. C., & Lee, S. R. (2023). Strategies for natural product discovery by unlocking cryptic biosynthetic gene clusters in fungi. *Separations, 10*(6), 333. [Crossref]

Ibrahim, H. I., Ibrahim, H. Y., Adeola, S. S., & Ojoko, E. A. (2022). Post-harvest loss and food security: A case study of major food crops in Katsina State, Nigeria. *FUDMA Journal of Agriculture and Agricultural Technology, 8*(1), 393–403. [Crossref]

Jomova, K., Raptova, R., Alomar, S. Y., Alwasel, S. H., Nepovimova, E., Kuca, K., & Valko, M. (2023). Reactive oxygen species, toxicity, oxidative stress, and antioxidants: Chronic diseases and aging. *Archives of Toxicology, 97*(10), 2499–2574. [Crossref]

Kankara, I. S., & Abdullahi, F. (2024). From Chibok Girls to Kankara Boys: An overview of parameters surrounding the kidnapping of Kankara school children in Katsina State, Nigeria 1987-2019. *International Journal of Research and Innovation in Social Science, 8*(2), 2341–2354. [Crossref]

Katiki, M., Neetu, N., Pratap, S., & Kumar, P. (2022). Biochemical and structural basis for *Moraxella catarrhalis* enoyl-acyl carrier protein reductase (FabI) inhibition by triclosan and estradiol. *Biochimie, 198*, 8–22. [Crossref]

Khattak, S. U., Lutfullah, G., Iqbal, Z., Ahmad, J., Rehman, I. U., Shi, Y., & Ikram, S. (2021). *Aspergillus flavus* originated pure compound as a potential antibacterial. *BMC Microbiology, 21*, 1–9. [Crossref]

Kumar, S., Mohan, A., Sharma, N. R., Kumar, A., Girdhar, M., Malik, T., & Verma, A. K. (2024). Computational frontiers in aptamer-based nanomedicine for precision therapeutics: A

comprehensive review. *ACS Omega, 9*(25), 26838–26862. [Crossref]

Lawal, M., Sharma, N. R., Verma, A. K., & Rakhra, G. (2025). Molecular modeling and identification of flax microgreens lignans as novel prostate cancer target inhibitors. *Journal of Applied Biology and Biotechnology, 13*(2), 242–257. [Crossref]

Lawal, M., Verma, A. K., Umar, I. A., Gadanya, A. M., Umar, B., Yahaya, N., & Auwal, B. (2020). Analysis of new potent anti-diabetic molecules from phytochemicals of *Pistia strateotes* with Sglt1 and G6pc proteins of *Homo sapiens* for treatment of diabetes mellitus: An in silico approach. *IOSR Journal of Pharmacy and Biological Sciences, 15*(4), 59–73. [Crossref]

Lin, P., Kook, M., Yi, T. H., & Yan, Z. F. (2023). Current fungal taxonomy and developments in the identification system. *Current Microbiology, 80*(12), 375. [Crossref]

Lipinski, C. A., Lombardo, F., Dominy, B. W., & Feeney, P. J. (1997). Experimental and computational approaches to estimate solubility and permeability in drug discovery and development settings. *Advanced Drug Delivery Reviews, 23*(1-3), 3–25. [Crossref]

Liu, R., Peng, X. P., Newman, D. J., Purchase, D., Li, G., & Kusari, S. (2025). Unlocking the metabolic potential of endophytic fungi through epigenetics: A paradigm shift for natural product discovery and plant-microbe interactions. *Natural Product Reports, 42*(10), 1690–1716. [Crossref]

Lykholat, Y. V., Khromykh, N. O., Didur, O. O., Drehval, O. A., Sklyar, T. V., & Anishchenko, A. O. (2021). *Chaenomeles speciosa* fruit endophytic fungi isolation and characterization of their antimicrobial activity and the secondary metabolites composition. *Beni-Suef University Journal of Basic and Applied Sciences, 10*, 1–10. [Crossref]

MacNair, C. R., Tsai, C. N., Rutherford, S. T., & Tan, M. W. (2023). Returning to nature for the next generation of antimicrobial therapeutics. *Antibiotics, 12*(8), 1267. [Crossref]

Maliehe, T. S., Mbambo, M., Nqotheni, M. I., Senzo, N. S., & Shandu, J. S. E. (2022). Antibacterial effect and mode of action of secondary metabolites from fungal endophyte associated with *Aloe ferox* Mill. *Microbiology Research, 13*(1), 90–101. [Crossref]

Mattoo, A. J., & Nonzom, S. (2021). Endophytic fungi: Understanding complex cross-talks. *Symbiosis, 83*(3), 237–264. [Crossref]

Mishra, S., Bhattacharjee, A., & Sharma, S. (2021). An ecological insight into the multifaceted world of plant-endophyte association. *Critical Reviews in Plant Sciences, 40*(2), 127–146. [Crossref]

Muthukrishnan, S., Prakathi, P., Sivakumar, T., Thiruvengadam, M., Jayaprakash, B., Baskar, V., & Shariati, M. A. (2022). Bioactive components and health potential of endophytic micro-fungal diversity in medicinal plants. *Antibiotics, 11*(11), 1533. [Crossref]

Nassar, A. R. A., Atta, H. M., Abdel-Rahman, M. A., El Naghy, W. S., & Fouda, A. (2023). Myco-synthesized copper oxide nanoparticles using harnessing metabolites of endophytic fungal strain *Aspergillus terreus*: An insight into antibacterial, anti-Candida, biocompatibility, anticancer, and antioxidant activities. *BMC Complementary Medicine and Therapies, 23*(1), 261. [Crossref]

Nhlapho, S., Nyathi, M. H. L., Ngwenya, B. L., Dube, T., Telukdarie, A., Munien, I., & Chude-Okonkwo, U. A. (2024). Druggability of pharmaceutical compounds using Lipinski rules with machine learning. *Sciences of Pharmacy, 3*(4), 177–192. [Crossref]

Niazi, S. K., Basavarajappa, D. S., Kumaraswamy, S. H., Bepari, A., Hiremath, H., Nagaraja, S. K., & Nayaka, S. (2023). GC-MS based characterization, antibacterial, antifungal and anti-oncogenic activity of ethyl acetate extract of *Aspergillus niger* strain AK-6 isolated from rhizospheric soil. *Current Issues in Molecular Biology, 45*(5), 3733–3756. [Crossref]

Nikolova, K., Popstoyanova, D., Dincheva, I., Gentscheva, G., Gerasimova, A., Panova, N., & Nicheva, D. (2025). Bioactive components in *Moringa oleifera* leaves and their 3D excitation-emission matrices, IR and Raman spectra. *Natural Product Communications, 20*(6), Article 1934578X251349296. [Crossref]

Nongthombam, K. S., Mutum, S. S., & Pandey, R. R. (2024). Secondary metabolite profiling of the endophytic fungus *Trichoderma longibrachiatum* L2D2 isolated from *Anaphalis contorta*. *Annual Research and Review in Biology, 39*(2), 1–15. [Crossref]

Osunde, O. M., Atere, C. T., Adesanwo, O. O., Taiwo, L. B., & Olayinka, A. (2024). FTIR characterization of bioactive functional groups present in crude extract of mycoherbicides produced from consortium culture of rhizosphere fungal isolates. *Communications in Soil Science and Plant Analysis, 55*(19), 2858–2867. [Crossref]

Pang, Z., Chen, J., Wang, T., Gao, C., Li, Z., Guo, L., & Cheng, Y. (2021). Linking plant secondary metabolites and plant microbiomes: A review. *Frontiers in Plant Science, 12*, Article 621276. [Crossref]

Pramitha, V. S., Sajeetha, S. B., Alsif, H., Aiswarya, A., Fathima, J. A. R., & Aryaraj, D. (2021). Characterization and bioactivity study of chitosan based nanomaterial from exoskeleton waste of *Parapaeneopsis stylifera* [Preprint]. Research Square. [Crossref]

Qadir, S. U., & Raja, V. (2021). Herbal medicine: Old practice and modern perspectives. In *Phytomedicine* (pp. 149–180). Academic Press. [Crossref]

Rai, N., Kumari Keshri, P., Verma, A., Kamble, S. C., Mishra, P., Barik, S., & Gautam, V. (2021). Plant associated fungal endophytes as a source of

natural bioactive compounds. *Mycology, 12*(3), 139–159. [Crossref]

Ramesh, M., Kavitha, K., Rajalakshmi, A., Anjukam, E., Prabakaran, V., Prakash, M., & Ramesh, B. (2022). 4a-methyl-dodecahydro-1H-pyrrolo [3, 4-b] quinoline-6-one produced by endophytic fungi *Aspergillus niger* E12 obtained from *Dodonaea viscosa* plant leaves as a novel antibacterial compound. *Applied Biochemistry and Biotechnology, 194*(11), 5132–5150. [Crossref]

Rani, R., Sharma, D., Chaturvedi, M., & Yadav, J. P. (2017). Antibacterial activity of twenty different endophytic fungi isolated from *Calotropis procera* and time kill assay. *Clinical Microbiology, 6*(3), 280. [Crossref]

Saini, P., Verma, A., Tiwari, H., Mishra, V., & Gautam, V. (2024). Omics-based approaches in studying fungal endophytes and their associated secondary metabolites. In *Endophytic fungi: The hidden sustainable jewels for the pharmaceutical and agricultural industries* (pp. 209–227). Springer International Publishing. [Crossref]

Salam, M. A., Al-Amin, M. Y., Salam, M. T., Pawar, J. S., Akhter, N., Rabaan, A. A., & Alqumber, M. A. (2023). Antimicrobial resistance: A growing serious threat for global public health. *Healthcare, 11*(13), 1946. [Crossref]

Salisu, B. U., Anua, S. M., Wan Rosli, W. I., & Mazlan, N. (2024). Bioburden, phenotypic and spectroscopic characterization of toxigenic and atoxigenic *Aspergillus* section *Flavi* from poultry feeds in Kelantan, Malaysia and Katsina, Nigeria. *Malaysian Journal of Microbiology, 20*(2), 120–131. [Crossref]

Salisu, B., Anua, M. S., Wan Ishak, W. R., & Mazlan, N. (2020). Incidence, distribution and phenotypic characterisation of aflatoxigenic fungi contaminating commonly consumed food grains in Katsina State, Nigeria. *Malaysian Journal of Medicine and Health Sciences, 16*(SUPP11), 103–111.

Salisu, B., Anua, M. S., Wan Ishak, W. R., & Mazlan, N. (2022a). An improved Fourier-Transform Infrared Spectroscopy combined with partial least squares regression for rapid quantification of total aflatoxins in commercial chicken feeds and food grains. *Journal of Advanced Veterinary and Animal Research, 9*(3), 546–564. [Crossref]

Salisu, B., Anua, M. S., Wan Ishak, W. R., & Mazlan, N. (2022b). Mycotoxigenic fungi contamination of grains and peanuts from open markets in Kelantan, Malaysia. *Food Research, 6*(1), 69–77. [Crossref]

Salisu, B., Anua, M. S., Wan Ishak, W. R., & Mazlan, N. (2024a). A polyphasic characterization of *Aspergillus* section *Flavi* isolated from Malaysian and Nigerian food grains and poultry feeds by phenotypic, chemotypic, and molecular methods. *Biocatalysis and Agricultural Biotechnology, 58*, Article 103217. [Crossref]

Satriawan, H., Zaimi, N. A., Eriadi, A., Efdi, M., Tallei, T. E., Andayani, R., & Handayani, D. (2025). Isolation and evaluation of the antimicrobial activity of endophytic fungi from *Orthosiphon aristatus*. *Biodiversitas Journal of Biological Diversity, 26*(2), 821–830. [Crossref]

Shehu, A. K. (2023). Isolation, identification, FT-IR spectroscopy and cytotoxicity of crude ethyl acetate extract of endophytic fungi (*Aspergillus niger*) isolated from rhizome of *Curcuma longa*. *Bayero Journal of Pure and Applied Sciences, 14*(1), 440–443. [Link]

Singh, P., Sharma, A., Bordoloi, M., & Nandi, S. P. (2020). Molecular identification of endophytic fungi isolated from medicinal plant. *Biointerface Research in Applied Chemistry, 10*(5), 6436–6443. [Crossref]

Spackman, P. R., Turner, M. J., McKinnon, J. J., Wolff, S. K., Grimwood, D. J., Jayatilaka, D., & Spackman, M. A. (2021). *CrystalExplorer*: A program for Hirshfeld surface analysis, visualization and quantitative analysis of molecular crystals. *Journal of Applied Crystallography, 54*(3), 1006–1011. [Crossref]

Thiele-Bruhn, S. (2021). The role of soils in provision of genetic, medicinal and biochemical resources. *Philosophical Transactions of the Royal Society B: Biological Sciences, 376*(1834), Article 20200183. [Crossref]

Tiwari, P., & Bae, H. (2022). Endophytic fungi: Key insights, emerging prospects, and challenges in natural product drug discovery. *Microorganisms, 10*(2), 360. [Crossref]

Tiwari, P., Thakkar, S., & Dufossé, L. (2025). Antimicrobials from endophytes as novel therapeutics to counter drug-resistant pathogens. *Critical Reviews in Biotechnology, 45*(1), 164–190. [Crossref]

Trabelsi, W., Fouzai, C., Telahigue, K., Chetoui, I., Nechi, S., Chelbi, E., & Soudani, N. (2023). The potential adverse effects of acrylamide on the oxidative stress response, fatty acids profile, and histopathological aspect of the Mediterranean *Holothuria forskali* respiratory tree. *Environmental Toxicology, 38*(1), 159–171. [Crossref]

Tripathi, M., & Agnihotri, V. (2024). Beyond the bark: Endophytic fungal diversity in *Taxus* spp. and their crucial role in medicinally relevant secondary metabolites. In *Ethnopharmacology and OMICS advances in medicinal plants volume 2: Revealing the secrets of medicinal plants* (pp. 117–135). Springer Nature Singapore. [Crossref]

Verma, A. K., Gulati, P., Lakshmi, G. B. V. S., Solanki, P. R., & Kumar, A. (2023). Interaction studies of gut metabolite trimethylene amine oxide with bovine serum albumin through spectroscopic, DFT and molecular docking approach. *bioRxiv*. [Crossref]

Verma, A., Shameem, N., Jatav, H. S., Sathyanarayana, E., Parray, J. A., Poczai, P., & Sayyed, R. Z. (2022). Fungal endophytes to combat biotic and abiotic stresses for climate-smart and sustainable agriculture. *Frontiers in Plant Science, 13*, Article 953836. [Crossref]

Wadhwa, K., Kapoor, N., Kaur, H., Abu-Seer, E. A., Tariq, M., Siddiqui, S., ... & Alghamdi, S. (2024). A comprehensive review of the diversity of

fungal secondary metabolites and their emerging applications in healthcare and environment. *Mycobiology, 52*(6), 335-387. [Crossref]

Wittayapipath, K., Laolit, S., Yenjai, C., Chio-Srichan, S., Pakarasang, M., Tavichakorntrakool, R., & Prariyachatigul, C. (2019). Analysis of xanthyletin and secondary metabolites from *Pseudomonas stutzeri* ST1302 and *Klebsiella pneumoniae* ST2501 against *Pythium insidiosum*. *BMC Microbiology, 19*(1), 78. [Crossref]

Zihad, S. N. K., Hasan, M. T., Sultana, M. S., Nath, S., Nahar, L., Rashid, M. A., & Shilpi, J. A. (2022). Isolation and characterization of antibacterial compounds from *Aspergillus fumigatus*: An endophytic fungus from a mangrove plant of the Sundarbans. *Evidence-Based Complementary and Alternative Medicine, 2022*(1), Article 9600079. [Crossref]